TTK4210 Advanced Control of Industrial Systems, Exercise 6

Kristian Løvland

Contents

1 Abstract **3**

2 Introduction **4**
2.1 Structure of the report 4
2.2 Problem summary 4

3 Secondary controllers **6**
3.1 The SIMC method 6
3.2 Tuning 6

4 Level controllers **11**
4.1 Notation 11
4.2 System identification and analysis 11
4.2.1 Experiment 11
4.2.2 Analysis 12
4.3 Controller tuning 13

5 Composition controllers **19**
5.1 System identification and analysis 19
5.1.1 Experiment 19
5.1.2 Analysis 20

6 Results **25**
6.1 PI controller tuning 25
6.2 Plots 25

A System identification experiments **33**
A.1 Open-loop responses of manipulated variables 33
A.2 System identification experiment for level control 33
A.3 System identification experiment for composition (temperature) control 33

1 Abstract

In this project, a model of a butane distillation column was used to design a controller for the composition of two product streams consisting of n-butane and iso-butane, respectively. By identifying characteristics of relevant subsystems, PI controllers for the states of these systems were designed with the ultimate goal of keeping the purity of the products at a satisfactory level. In the end, quick control without excessive oscillation was acheived.

2 Introduction

2.1 Structure of the report

The system analysis, controller design, controller tuning and results are presented in the order they were done. All experiments referred to when doing system identification are plotted in the appendix to avoid drowning the reader in plots. Matlab code is included where it was considered necessary.

2.2 Problem summary

A good introduction to the control problem we're faced with is given in the assignment text [1]. A short summary follows.

The top product is required to contain no more than 4% n-butane, while the bottom product is required to contain less than 2,5% iso-butane.

These compositions, denoted x_D^* and x_B^*, are in practice controlled through their temperatures. These are measured on the top and bottom of the distillation column, and are denoted T_D and T_B. The temperature needed to acheive the required compositions are shown in table 1, together with the actual temperature setpoint. These are a bit lower/higher than than strictly necessary to introduce a safety margin.

	Required temperature	Temperature setpoint
Top product (D)	$35,85°$ C	$35,30°$ C
Bottom product (B)	$47,69°$ C	$48,51°$ C

Table 1: Temperatures giving satisfactory product quality

To satisfy these specifications, the rest of the states in the system need to stay in reasonable areas. This means levels M_D in the top accumulator and M_B in the distillation column, together with distillation column pressure p, need to be controlled stably to their setpoints.

To control these five variables, five degrees of freedom is needed. Our five manipulated variables are flow rates in different parts of the system, denoted V_T, L, D, V and B. Each of these are controlled by their own inputs, mostly valves.

Table 2 shows the pairing of manipulated and controlled variables. As mentioned, it is assumed that choosing good setpoints for T_D and T_B gives

satisfactory product quality. This control structure is called LV-control, after the manipulated variables used to control product quality.

Manipulated Variable	V_T	D	B	L	V
Controlled variable	p	M_D	M_B	T_D	T_B

Table 2: Variable pairings

3 Secondary controllers

The secondary controllers were tuned individually using the SIMC method for PI controllers. A step in process input of 50% of maximum input was used for all the secondary controllers controlling the states D, L, B and p. For V, a step input change of 20% was used to avoid effects from other parts of the system.

3.1 The SIMC method

A summary of the SIMC method is given in [3]. The method assumes that the system can be approximated by a first order process with time delay, which has transfer function

$$G(s) = \frac{ke^{-\theta s}}{1 + T_1 s} \tag{1}$$

This system is to be controlled by a PI controller

$$K(s) = K_p \frac{1 + T_i s}{T_i s} \tag{2}$$

The SIMC method gives rules for choosing K_p and T_i, given a desired closed-loop time contant T_L. The two steps of the method are then

1. Fit the step response to a first order model. This means finding time delay θ, slope $k' = \frac{dy/dt}{\Delta u}$ and time constant T_1 from the plot of the step response.

2. To achieve the desired time constant T_L, use the PI controller parameters $K_p = \frac{1}{k'} \frac{1}{\tau + T_L}$, $T_i = \min(T_1, 4(\tau + T_L))$.

How one chooses T_L depends on the desired response. In [3], $T_L = 0.3\tau$ is suggested for "aggressive" control. If no overshoot is desired, one should choose $T_L > 2\tau$.

3.2 Tuning

The step experiments can be seen in figures 27, 28, 29, 30 and 31. The reference signals should have been omitted from these plots since we are dealing with open loop systems, and can safely be ignored here.

The plots show that for the first three variables, the accuracy of the simulation is clearly not sufficient for fitting a first order model (they behave in a stepwise fashion). Inspecting the orders of magnitude of the gains and time constants may however still be useful. To approximate their sizes, a straight line was drawn from initial state to steady-state. Its slope was considered to be $\frac{dy}{dt}$, and the point where this line crossed 63% of the change was considered to be the time constant. This method clearly causes underestimates of $\frac{dy}{dt}$ and overestimates of T_1, but it's hard to find a meaningful way to fit a tangent given the insufficient information. For the two other variables, more reasonable readings could be done. All results are shown in table 3.

Our desired time constant T_L for each loop is shown in the table as well. Initially, $T_L = 0,3\tau$ was chosen for the three fastest loops. Some simple trial and error in K-spice showed that this lead to oscillation and unfortunate interaction between control loops, especially the controllers for D and L. This is probably partly due to the underestimates of k' and T_1 for these variables. Conservative estimates of these results in more aggressive controllers (to compensate for the slow system) when using the SIMC method.

Due to this unsatisfactory behaviour, $T_L = 2\tau$ was chosen for the three fastest control loops instead. The time delay was hard to make a meaningful reading of for the two other systems, so a somewhat arbitrary choice of $T_L = 10s$ was chosen for these systems (instead of using the $T_L = 2\tau$ rule). Like all the other parameters, these were not absolute choices, but a good starting point for further tuning.

After calculating the SIMC controller values, some more qualitative tuning using K-spice simulations was not surprisingly needed. For D and L, the integral times were kept fixed, while the gain needed to be decreased to avoid oscillations. For B, it was necessary to reduce the integral time in addition to reducing the gain to avoid oscillation. The response of V was slow, and to avoid bandwith limitations in the control of T_B later, both controller parameters were changed to give dramatically more aggressive behaviour. For p, the stationary deviation was initially removed pretty slowly, so the integral time was reduced, while also reducing gain to avoid oscillation.

The results of implementing these controllers in K-spice, using the internally scaled gain $G = K_p \frac{(y_{\max} - y_{\min})}{(u_{\max} - u_{\min})}$ for all controllers, are shown in figures 1, 2, 3, 4 and 5.

	τ	T_1	$\frac{dy}{dt}$	Δu	k'	T_L
D	1,0s	0,4s	14,3	50%	28,6	2s
L	1,0s	1,0s	47,5	50%	95,0	2s
B	1,0s	0,6s	10,0	50%	20,0	2s
V	≈ 0	400s	0,028	20%	0,14	10s
p	≈ 0	200s	0,088	50%	0,18	10s

Table 3: Identified parameters for inner loop

	$K_{p,\text{SIMC}}$	$T_{i,\text{SIMC}}$	$K_{p,\text{final}}$	$T_{i,\text{final}}$
D	0,012	0,4s	0,0035	0,4s
L	0,035	1,0s	0,0018	1,0s
B	0,016	0,6s	0,0025	1,0s
V	0,71	40s	1,65	10s
p	0,57	40s	0,25	20s

Table 4: PI controller parameters for inner loop

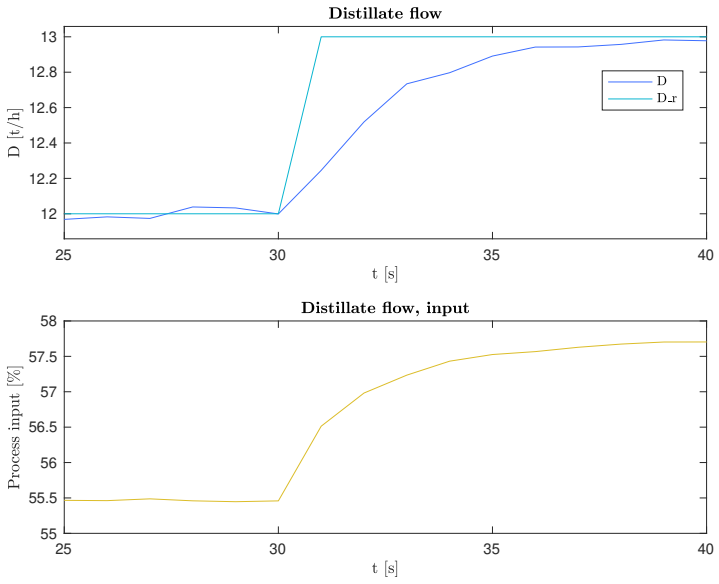

Fig. 1: Closed-loop step response of D

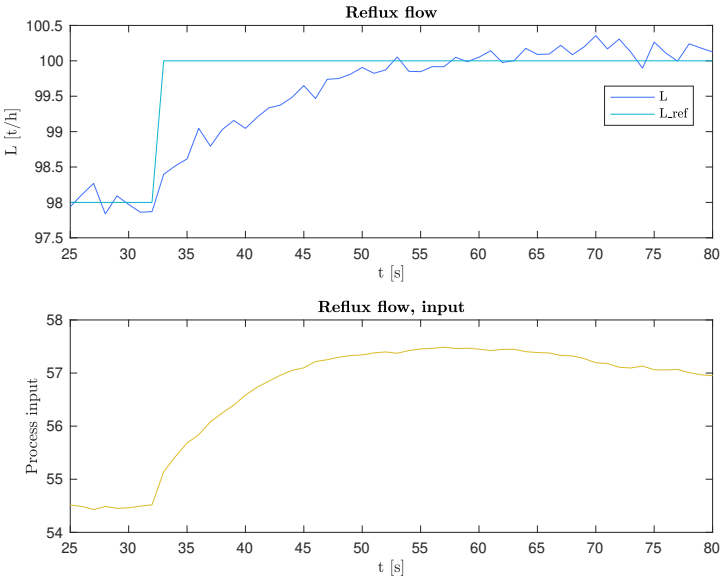

Fig. 2: Closed-loop step response of L

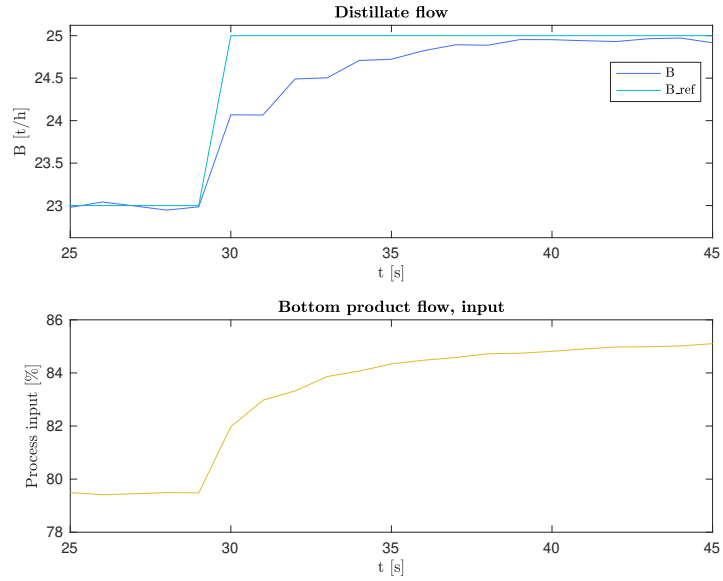

Fig. 3: Closed-loop step response of B

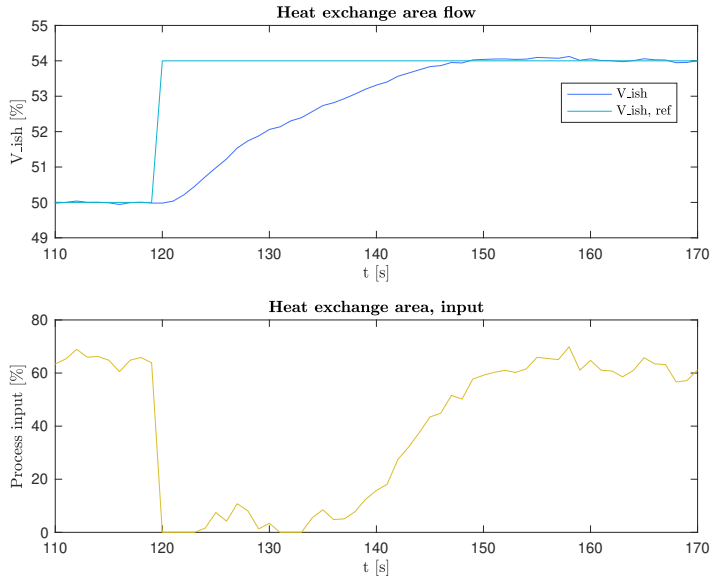

Fig. 4: Closed-loop step response of heat exchanger area, related to V

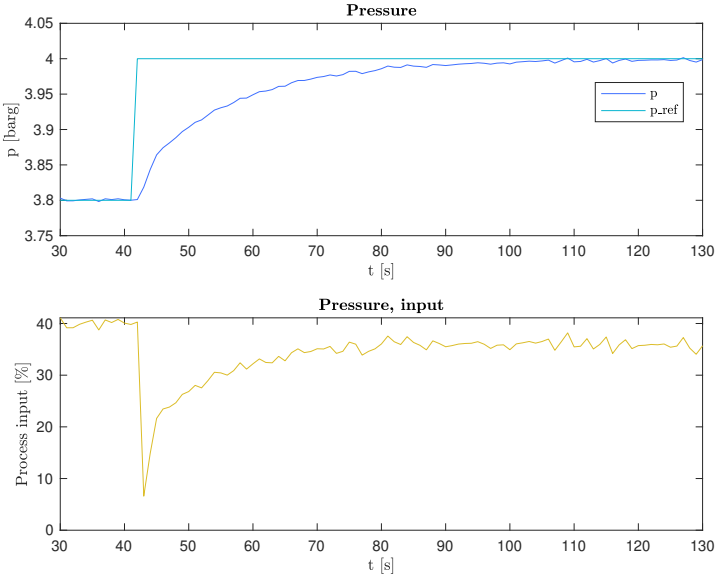

Fig. 5: Closed-loop step response of p

4 Level controllers

The level controllers were identified using the `d-sr` toolbox on the closed-loop responses of the level control loops in the reflux drum, and in the distillation column.

4.1 Notation

The system being analysed in the sectioon consists of the input $u = [D \quad B]^T$, the state $y = [M_D \quad M_B]^T$ and the reference $r = [M_{D,\text{ref}} \quad M_{B,\text{ref}}]^T$. By exciting the controlled system

$$y(s) = L(s)e(s) = G(s)K(s)(y(s) - r(s)) \tag{3}$$

with changes in r, the loop transfer function $L(s) = \frac{y}{e}(s)$ may be identified. Choosing $K(s)$ to be diagonal during the identification experiment makes further analysis and controller tuning easier.

4.2 System identification and analysis

4.2.1 Experiment

The level controllers in the distillation column and reflux drum were expected to be more or less independent, but MIMO identification with `d-sr` was used anyway, due to the convenience of being able to reuse code in the composition control task. Data from K-spice was imported using the script delivered together with the assignment. This data was then analyzed using the following Matlab code

```
% State vector is y = [M_D; M_B], with corresponding input u = [D; B];
Y = [LC1016(:, 1), LC1015(:, 1)];
U = [LC1016(:, 2)-LC1016(:, 1), LC1015(:, 2)-LC1015(:, 1)];
% Dimensional limit parameter
L = 3;

[A,B,C,D,CF,F,x0]=dsr(Y,U,L);
```

The discrete-time system returned from `d-sr` was then transformed to the loop transfer function used in frequency analysis below by the following code

```
sample_time = min(diff(Time));
disc_system = ss(A, B, C, D, sample_time);
cont_system = d2c(disc_system);

A = cont_system.A;
B = cont_system.B;
C = cont_system.C;
D = cont_system.D;

[G_i1_num, G_i1_den] = ss2tf(A, B, C, D, 1);
[G_i2_num, G_i2_den] = ss2tf(A, B, C, D, 2);

l11 = tf(G_i1_num(1, :), G_i1_den);
l12 = tf(G_i2_num(1, :), G_i2_den);
l21 = tf(G_i1_num(2, :), G_i1_den);
l22 = tf(G_i2_num(2, :), G_i2_den);

L = [l11 l12; l21 l22];
RGA = L .* inv(L).';
```

The system was excited by step changes in references for M_D and M_B, which were controlled with P controllers, both with $K_p = 1200$. The references were changed at different periods, to better extract information about all frequencies. The states were attempted held in a reasonable interval, to avoid nonlinear effects such as saturation. The experiments are shown in figures 32 and 33.

4.2.2 Analysis

The identified model was chosen to have order 2, which is natural for what was expected to be a diagonal system with two variables. The interactions of the resulting system is shown in figure 6, which show the RGA of the identified $G(s)$. Inspecting this plot shows that the magnitudes of the off-diagonal elements are negligible at frequencies above $10^{-3}\frac{\text{rad}}{\text{s}}$. We shall see that this is well below the bandwith frequencies of the two loops. The diagonal elements of the RGA however, have gain close to unity at the bandwith frequencies. From here, the level controller system is considered to be diagonal, and the control loops are tuned independently using SISO methods.

Continuing using MIMO notation, a diagonal controller

$$K(s) = \begin{bmatrix} k_1(s) & 0 \\ 0 & k_2(s) \end{bmatrix} \tag{4}$$

with PI controllers $k_1(s)$ and $k_2(s)$ is designed based on the diagonal elements in the identified $G(s)$.

Figures 7 and 8 show the Bode plots of the transfer functions in the diagonals of the identified model. Note that these correspond to the loop transfer function $G(s)K(s)$ using a P controller with $K_p = 1200$. The controller derived here therefore has to be multiplied with this existing $K(s)$ when implemented.

Ignoring the 360° error in phase in the plots, the gain margin of loop transfer function $l_{11}(s) = \frac{M_D}{M_{D,ref}}(s)$ may be found to be to be 6,74dB as $\omega \to \infty$. Likewise, the gain margin of $l_{22}(s) = \frac{M_B}{M_{B,ref}}(s)$ is read to be 10,7dB as $\omega \to \infty$. Using the 6dB gain margin rule of thumb (which is often used in [3]), $K_{p,D}$ should not be increased by any significant amount, while $K_{p,B}$ might be increased by a factor of $10^{(10,7-6)/20} \approx 1,7$, yielding the controller gain $K_{p,B} = 2000$.

The phase plot of l_{11} shows that the integral part of the controller should be active in the lower frequency spectrum. To avoid the phase crossing the $-180°$ line, the choice of $T_i = 5000s$ is made. The phase response of l_{22} is pretty similar to the one of l_{11}, so initially choosing the same integral time for control of M_B should be reasonable.

Figures 9 and 10 show the magnitudes of the sensitivity functions for the two systems using these controllers. The distillation column is, not surprisingly, the hardest system of the two to control quickly. One might wish to push the bandwith of the M_B loop further to the right, but inspecting the phase plot again suggests not to attempt this. This is because the phase margin would be dangerously low K_p was increased or T_i was decreased, and the system would become more sensitive to time delays and similar phenomena. Disturbances at frequencies above $0,005\frac{\text{rad}}{\text{s}}$ should hopefully not be common in this system anyway.

4.3 Controller tuning

Simulation in K-spice showed stationary deviation in M_D. To counteract this, the integral time was reduced. Control of M_B worked satisfactory using the PI controller derived from the frequency analysis above. The slow

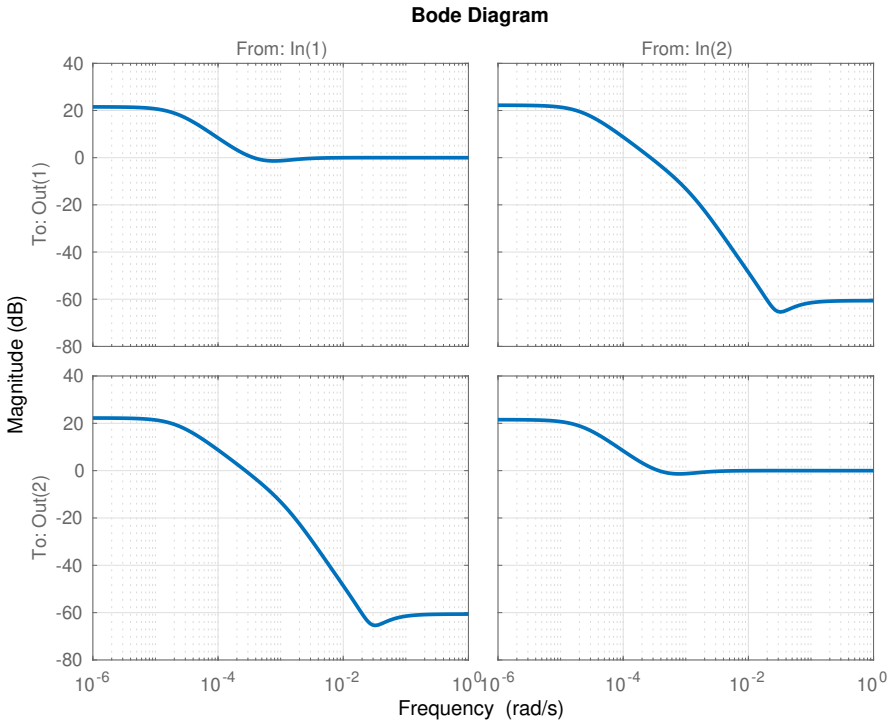

Fig. 6: Magnitude of RGA of identified BD system

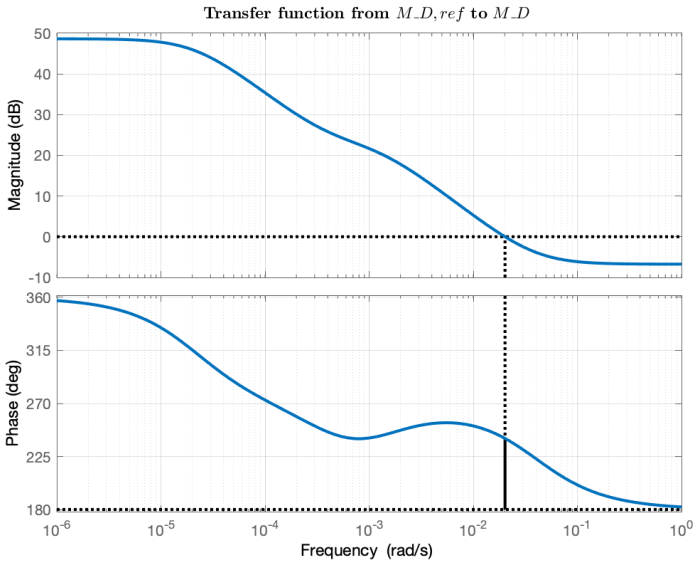

Fig. 7: Magnitude and phase response of reflux drum level from reflux drum level reference

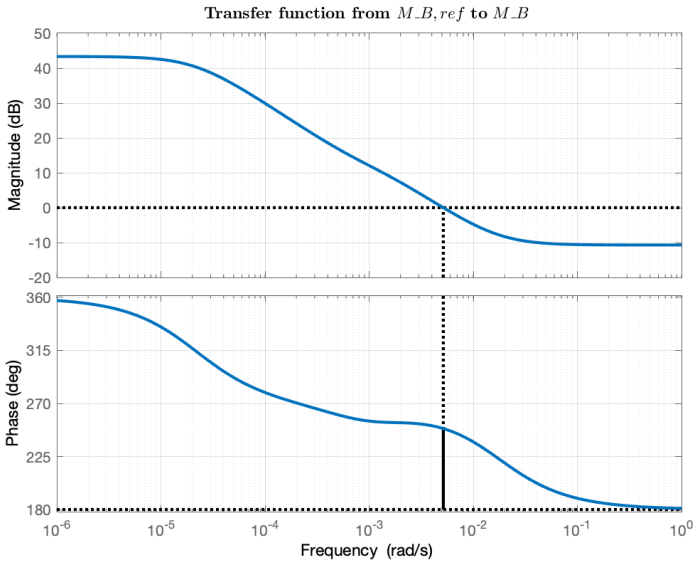

Fig. 8: Magnitude and phase response of distillation column level from distillation column level reference

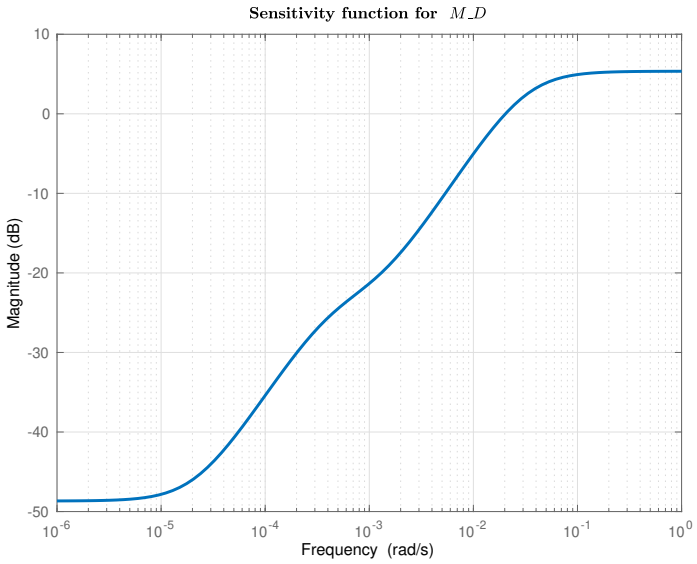

Fig. 9: Sensitivity function for reflux drum level control

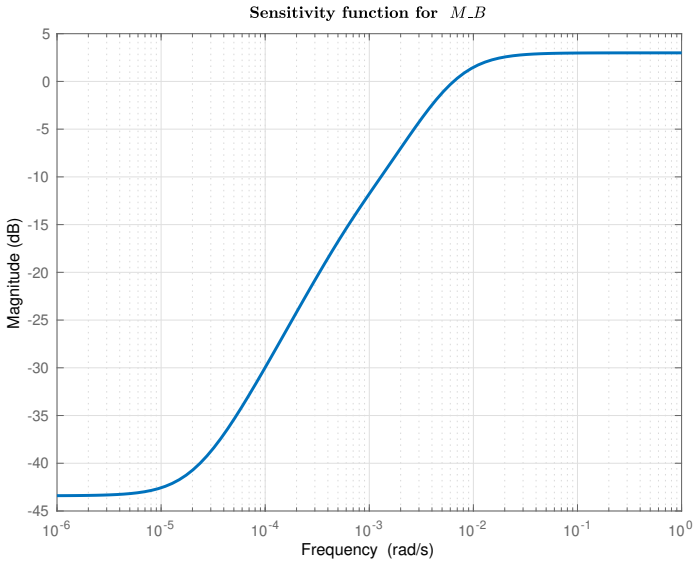

Fig. 10: Sensitivity function for distillation column level control

time constants of these systems combined with the complexity of the K-spice model, made tuning based on the K-spice model unpractical. It's natural to believe that access to more computing power would make it possible to find better controller parameters, but the controllers derived in from the analysis above didn't seem to be too terrible.

The initial parameters based on loop-shaping, and the final ones are shown in table 5. The step responses of the controlled levels are shown in figures 11 and 12.

	$K_{p,\text{initial}}$	$T_{i,\text{initial}}$	$K_{p,\text{final}}$	$T_{i,\text{final}}$
M_D	1200	5000s	1200	1000s
M_B	2000	5000s	2000	5000s

Table 5: Parameters for level controllers

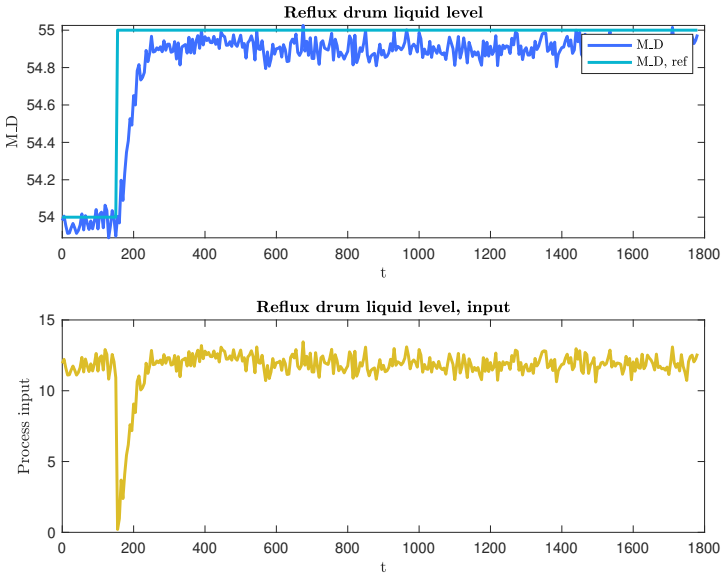

Fig. 11: Step response of controlled M_D

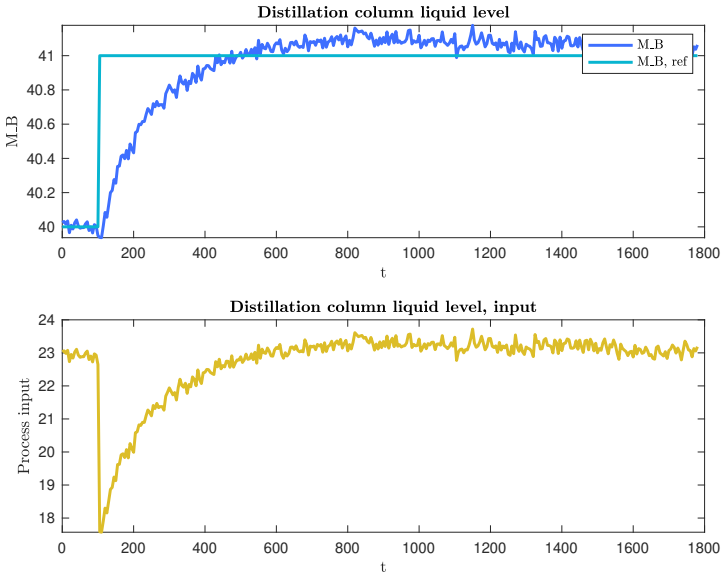

Fig. 12: Step response of controlled M_B

5 Composition controllers

Let $y = [T_D \quad T_B]^T$, $r = [T_{D,\text{ref}} \quad T_{B,\text{ref}}]^T$ and $u = [L \quad V]^T$. By changing the setpoints for the manipulated variables L and V, the system transfer function

$$G(s) = \frac{y}{u}(s) \tag{5}$$

may be identified directly.

5.1 System identification and analysis

5.1.1 Experiment

Identification of the LV system was done in a similar manner as in the previous section, using step changes in input (but open-loop this time). Again, `d-sr` was used for identification. The periods of the step changes were chosen more systematically than in the level experiment, with periods of 5 minutes, 15 minutes and ≈ 2 minutes being used for different periods of time. This was done to get an accurate representation of the system at all frequencies. The inputs L and V were changed alternatingly (i.e. 90° out of phase), to avoid ambiguity in which input caused what effects. Figure 34 shows the inputs (L and V) and resulting outputs (T_D and T_B) in the experiment. Simlarly to the previous section, the code used for identification was as follows

```
% State vector is y = [T_D; T_B], with corresponding input u = [L; V];
Y = [TC1015(:, 1), TC1088(:, 1)];
U = [FC1015(:, 1), LC1028(:, 1)];

% Scaling is done to keep all signals in the range [0, 1]
Y = (Y - 25*ones(size(Y))) * [1/25 0; 0 1/25];
U = U * [1/120 0; 0 1/100];

% Dimensional limit parameter
G = 3;

[A,B,C,D,CF,F,x0]=dsr(Y,U,G);
```

The code used to get the system transfer function $G(s)$ was identical to the code used in the previous system.

5.1.2 Analysis

Figure 13 shows the RGA of the identified system $G(s) = \frac{y}{u}(s)$. The chosen pairing is clearly the most reasonable. The interactions doesn't seem to be any problem, but the RGA doesn't tell the whole story. There is reason to believe that temperature in the bottom affects temperature in the top, and the right tool for this analysis is the *Performance Relative Gain Array* (PRGA).

Let $\tilde{G} = \text{diag}\{g_{ii}\}$, i.e. the matrix consisting of only the diagonal elements of the system matrix. This matrix is a useful tool for analysing interactions, and is used in the definition of the PRGA

$$\Gamma = \tilde{G}G^{-1} \tag{6}$$

This matrix is used as a measure of interaction. It is scaling dependent, so before any further analysis is done, this has to be taken into account. Given a subsystem

$$e = y - r = G(s)u + G_d(s)d - r \tag{7}$$

the signals should be scaled such that the maximum expected disturbance and maximum acceptable error both are of magnitude one. Table 7 shows the range used in K-spice for the states in the temperature control loops, and maximum accepted error. To be clear, the following analysis holds for both control loops, with y being temperature, r reference temperature, and u process input. The maximum error allowed is chosen based on the lowest margin proposed in the assignment text. Disturbance rejection is not considered because it is assumed that no disturbance will be greater than the disturbance coming from interaction between the loops. This effect is handled if we manage to keep $|e| < 1$.

The PRGA using this scaling is shown in figure 14. It is now clear that one can't simply choose a bandwith of $0,01\frac{\text{rad}}{\text{s}}$ and call it a day, since the interaction from V to T_D has its peak at this frequency.

What should be done, then? Since we're dealing with a MIMO system, only using the diagonal parts of G for designing controllers won't suffice. Our main objectives is to follow the reference. In [2], some rules for designing independent controllers for MIMO systems are proposed. One of these considers reference tracking, and is used here.

For effecient reference tracking in a SISO system, an error magnitude $|e(j\omega)|$ less than one is achieved when

$$|S(j\omega)R| < 1 \tag{8}$$

for reference changes of magnitude R, for all frequencies ω up to the maximum frequency ω_r where good reference tracking is required. More explicitly, this requirement can be stated as

$$|1 + L(j\omega)| > R \tag{9}$$

The situation for a MIMO system is a bit more complicated when we have interactions like shown above. This is where the PRGA is useful. It is shown in [2] that the MIMO analogue of equation 9 can be stated, using the PRGA, as

$$|1 + L_i| > |\gamma_{ij}| \cdot |R_j| \tag{10}$$

Here, $L_i = g_{ii}k_i$ is the loop transfer function in loop i, and R_j is the magnitude of the reference change in loop j.

Assuming $R_1 = R_2 = 1$ (which should hold for our rescaled system), the requirements are as plotted in figures 15 and 17, using $L_i = G_i$ (P controllers with unit gain). Inspecting these, it becomes clear that the state most desperately in need of better control is T_D. This is not surprising, since the PRGA showed the effect of T_B on T_D being large, while the effect the other way was more or less negligible. Hence, suppressing the effects T_B has on T_D is our most important task, while the control of T_B should be relatively problem free if the controller parameters aren't chosen completely ridiculously. To shape $|1+L_1|$, the integral time was first changed. $T_i = 100$s turned out to give a low maximum distance between $|1 + L_1|$ and $|\gamma_{1i}|$. K_p was then chosen to be as small as possible while still satisfying the criterion, yielding $K_p = 12$. This actually satisfies the criterion at all frequencies, as shown in 16.

The restriction of the T_B loop being located in a higher part of the frequency spectrum gave rise to the choice of $T_i = 1000s$ for this PI controller. Though the PRGA didn't suggest interaction from T_D to T_B would be a problem, the loop was designed to respect the inequality $|1 + L_2| > |\gamma_{22}|$ for all $\omega < 10^{-2}$ (meaning interaction from T_D should be suppressed). As shown in figure 18 is satisfied when $K_p = 25$. A summary of the resulting controller is shown in table 6

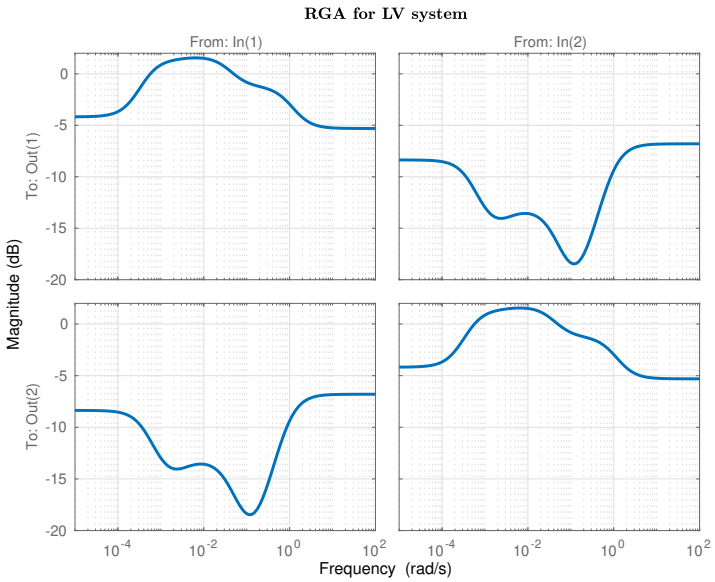

Fig. 13: RGA for LV system

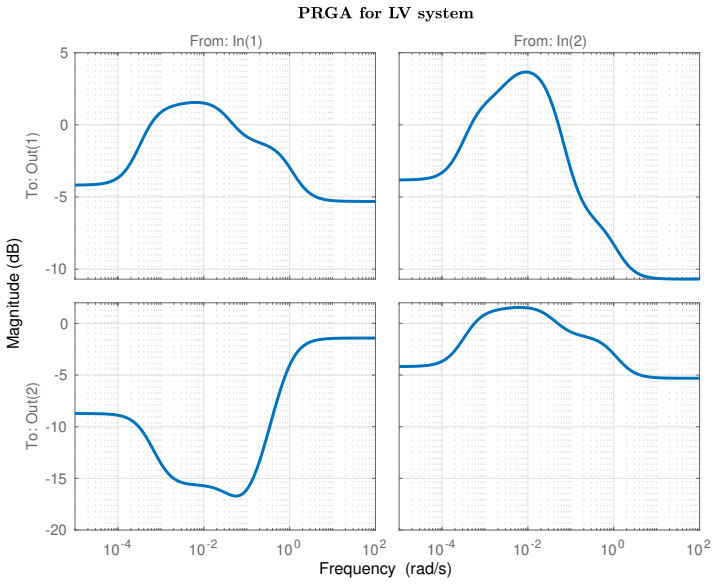

Fig. 14: PRGA for LV system

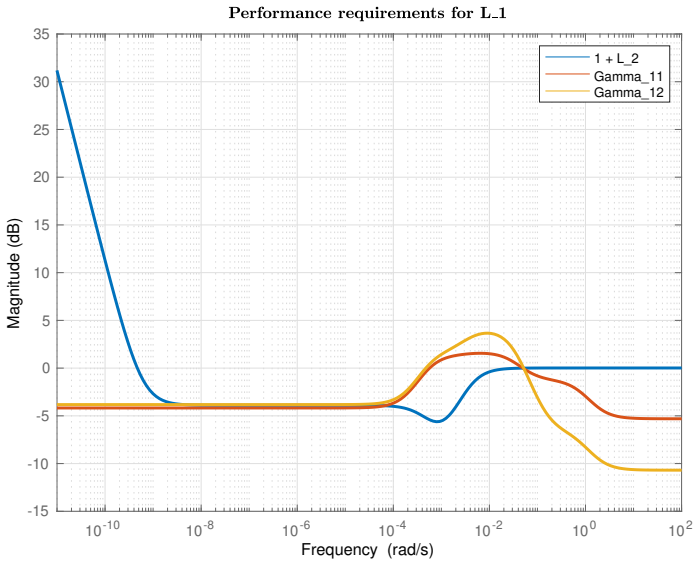

Fig. 15: Performance requirements for T_D loop, with unit gain P controller

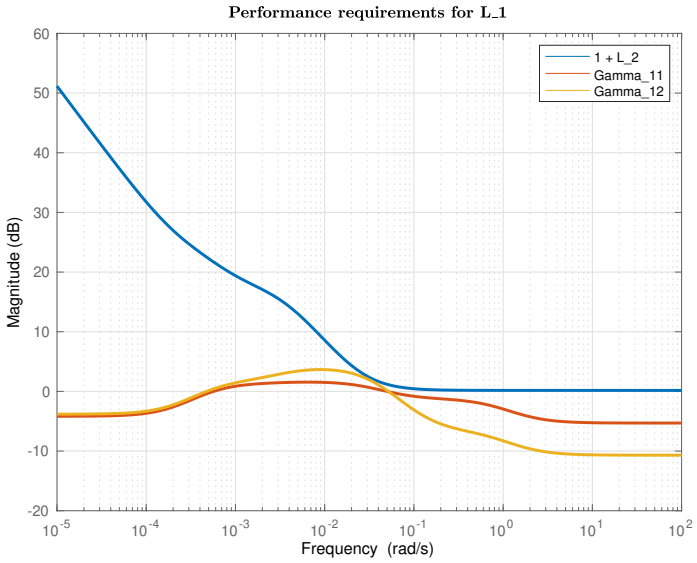

Fig. 16: Performance requirements for T_D loop, with implemented PI controller

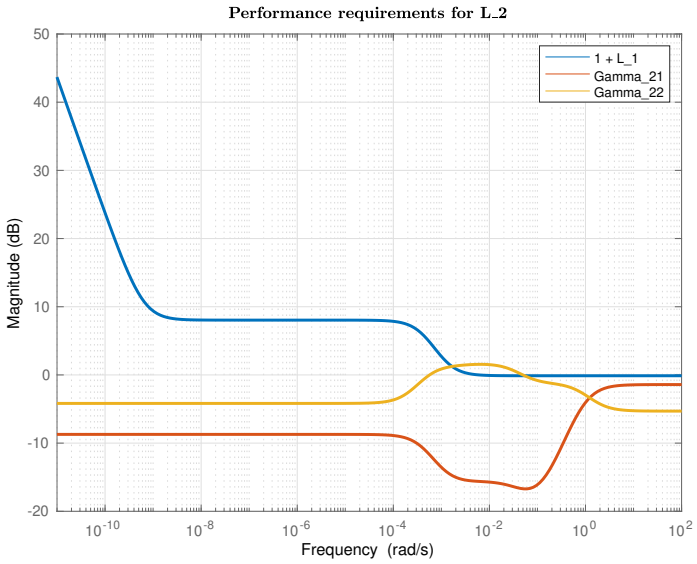

Fig. 17: Performance requirements for T_B loop, with unit gain P controller

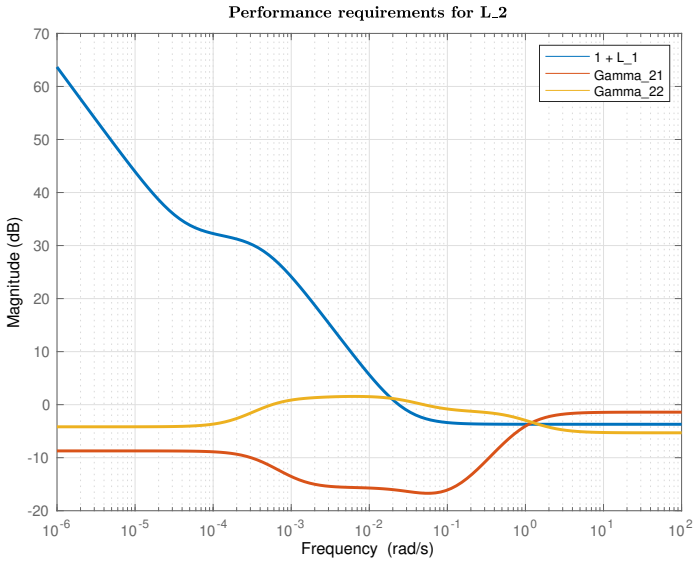

Fig. 18: Performance requirements for T_B loop, with implemented PI controller

	K_p	T_i
T_D	12	100s
T_B	25	1000s

Table 6: Parameters for temperature controllers

6 Results

6.1 PI controller tuning

Table 8 shows the final PI controller parameters for all the control loops tuned in this project, also including the scaled gain G used in the K-spice implementation.

6.2 Plots

Figures 19, 20, 21 and 22 show the results of relatively large step changes in temperature reference. The system is in both cases initially operating at the least strict setpoint required to keep the product streams sufficiently pure, and one of the temperatures is then suddenly changed to the setpoint given in the rightmost column of 1.

The plots show that there's clearly interactions in play here. However, the attempt at separating the responses in frequency seems to work. When$T_{B,\text{ref}}$ is increased, T_D also increases. However, the T_D controller quickly steers the state back to the reference, and keeps it there. This has the effect of disturbing the T_B loop again, but this is the last of the interactions here. After this minor set-back, T_B climbs steadily to its reference, and stays there.

A more dramatic effect is seen when T_D is changed. The T_B controller doesn't have the bandwith necessary suppress disturbances as quick as the step response of T_D. Instead, we have to rely on the interaction from T_D to T_B being low. The interaction is stronger stronger than what the PRGA suggested, and the disturbance causes a pretty long-lasting oscillation. Luckily, the magnitude of the oscillation is lower than the magnitude of the change in $T_{D,\text{ref}}$, and T_B is always high enough to keep product quality satisfactory.

Though the results seem ok, there are some possible problems. The greatest one is probably the long-lasting effects of interaction from T_D to T_B. Though the controllers could be tuned less aggressively to avoid rapid responses, this would also decrease disturbance suppression. An easier solu-

Variable	Min	Max	Maximum magnitude
T_D	25°C	50°C	25°C
T_B	25°C	50°C	25°C
$T_{D,\text{ref}}$	25°C	50°C	25°C
$T_{B,\text{ref}}$	25°C	50°C	25°C
L	$0\frac{\text{t}}{\text{h}}$	$120\frac{\text{t}}{\text{h}}$	$120\frac{\text{t}}{\text{h}}$
V	0%	100%	100%
e	-	-	$0,55$°C

Table 7: Scaling used in LV system analysis

	K_p	G	T_i
D (FC1005)	0,0035	0,42	0,4s
L (FC1015)	0,0018	0,22	1,0s
B (FC1019)	0,0025	0,3	1,0s
V (LC1028)	200	200	10s
p (PC1024)	5	30	20s
M_D (LC1016)	1200	10	1000s
M_B (LC1015)	2000	16,7	5000s
T_D (TC1015)	12	2,5	100s
T_B (TC1088)	25	6,3	1000s

Table 8: Final controller parameters

tion is to simply change the reference slower. Figures 23, 24, 25, 26 show the same experiments as was just discussed, but with smaller, stepwise changes to the reference. The effects the change in $T_{B,\text{ref}}$ has on T_D is reduced from $0,45°\text{C}$ to about $0,10°\text{C}$. Decreasing $T_{D,\text{ref}}$ stepwise causes T_B to oscillate with a magnitude of $0,10°\text{C}$ rather than $0,30°\text{C}$.

This type of slow setpoint change might for instance be implemented in practice by lowpass filtering the setpoint step changes. With this implemented, the relatively aggressive controllers derived here might be kept unchanged without risking instability. This has the advantage of keeping the relatively fast settling times seen here, of around 1,5 hours for both loops.

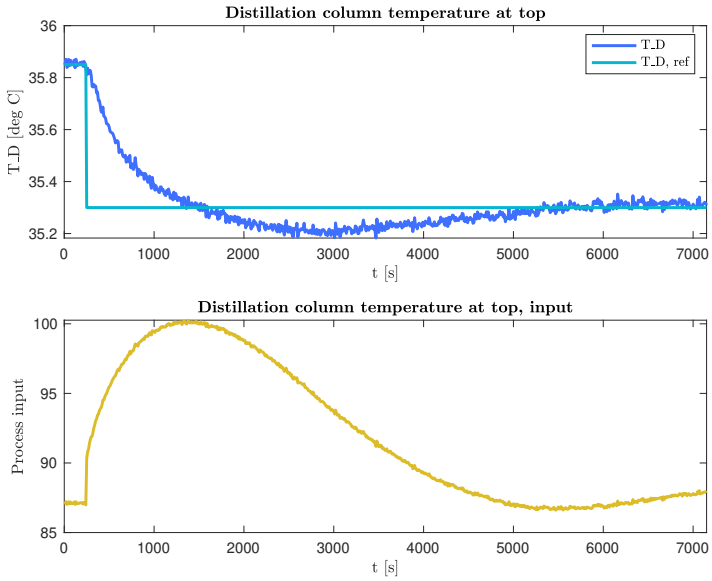

Fig. 19: Response of controlled T_D to step change in $T_{D,\text{ref}}$

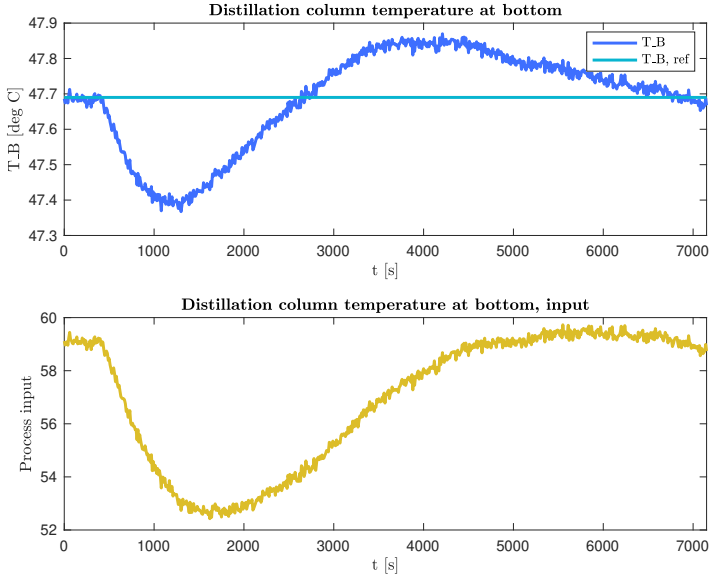

Fig. 20: Response of controlled T_B to step change in $T_{D,\text{ref}}$

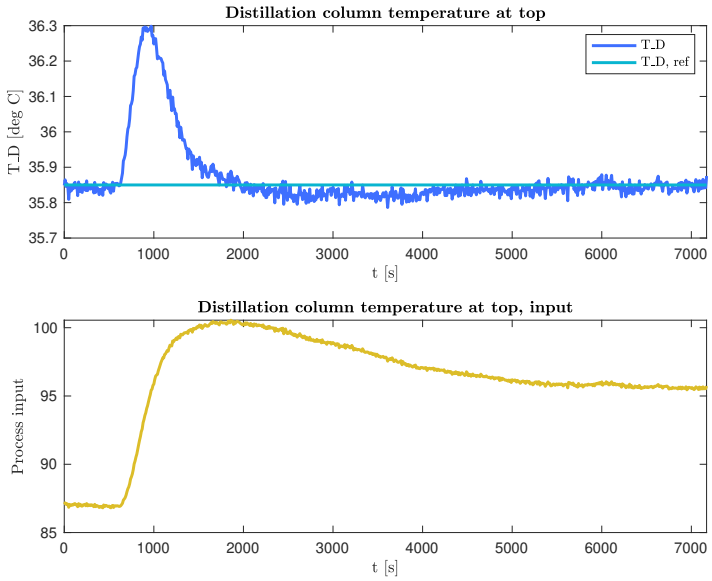

Fig. 21: Response of controlled T_D to step change in $T_{B,\text{ref}}$

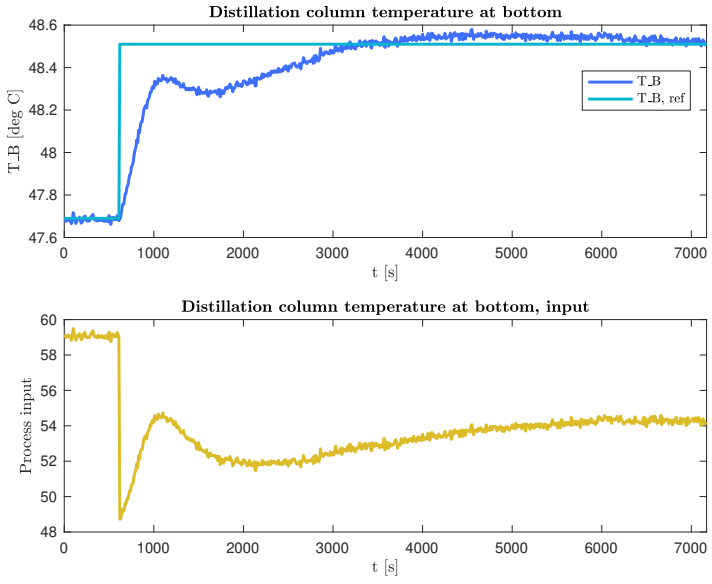

Fig. 22: Response of controlled T_B to step change in $T_{B,\text{ref}}$

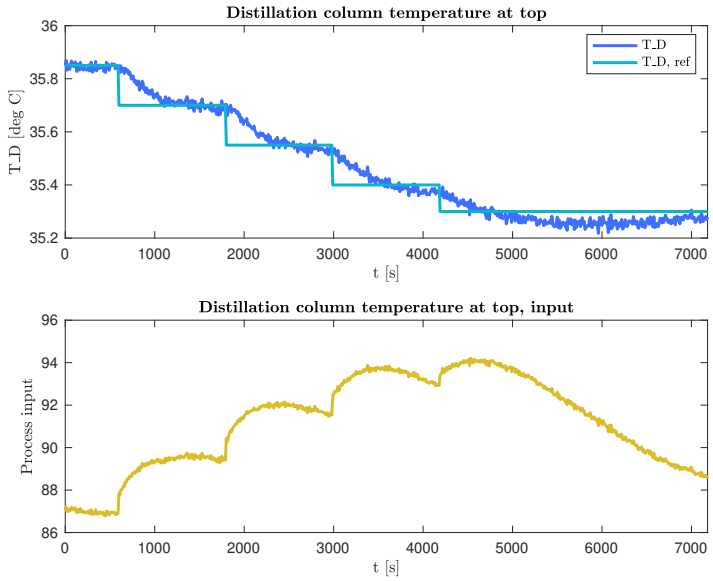

Fig. 23: Response of controlled T_D to stepwise step changes in $T_{D,\text{ref}}$

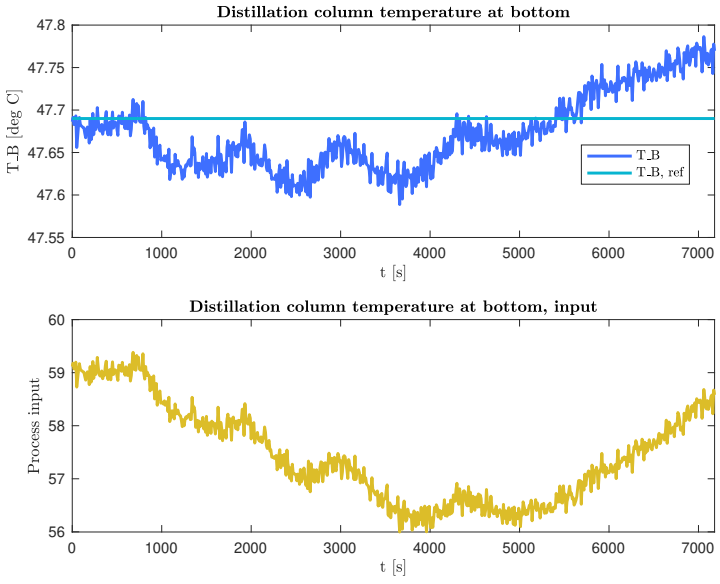

Fig. 24: Response of controlled T_B to stepwise step changes in $T_{D,\text{ref}}$

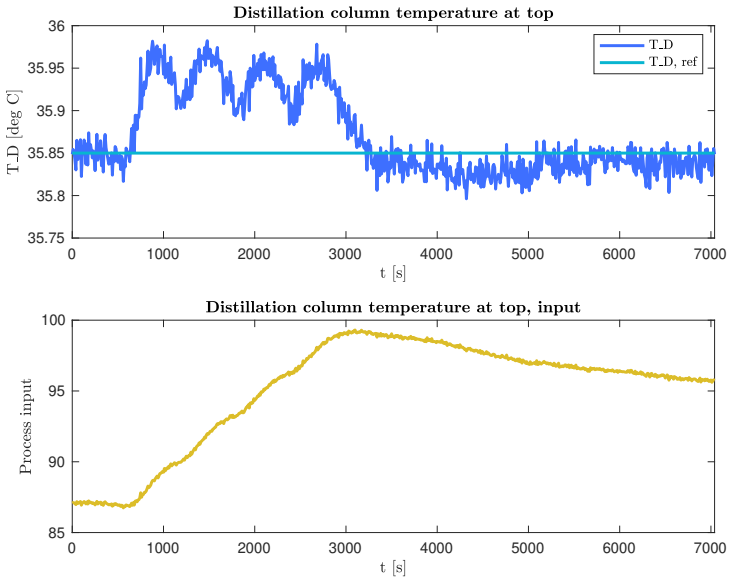

Fig. 25: Response of controlled T_D to stepwise step changes in $T_{B,\text{ref}}$

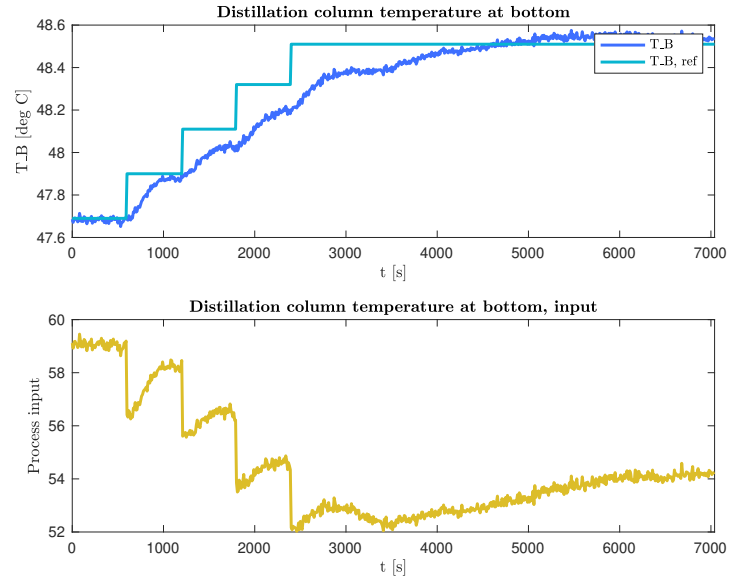

Fig. 26: Response of controlled T_B to stepwise step changes in $T_{B,\text{ref}}$

7 Conclusion

The control loops of the butane splitter was tuned to give stable responses, and for reasonable setpoints and setpoint changes, the temperature controllers should work satisfactory for the given requirements. The butane leaving Kårstø may safely be expected to adhere to specifications.

References

[1] Morten Hovd, *TTK4210 Advanced Control of Industrial Processes, Assignment 6*, 2020.

[2] Sigurd Skogestad and Ian Postlethwaite, *Multivariable Feedback Control*, John Wiley & Sons Ltd, Chichester, 2nd edition, 2005.

[3] Jens G. Balchen, Trond Andresen and Bjarne A. Foss, *Reguleringsteknikk*, Institutt for Teknisk Kybernetikk, Trondheim, 6th edition, 2016.

A System identification experiments

A.1 Open-loop responses of manipulated variables

A.2 System identification experiment for level control

A.3 System identification experiment for composition (temperature) control

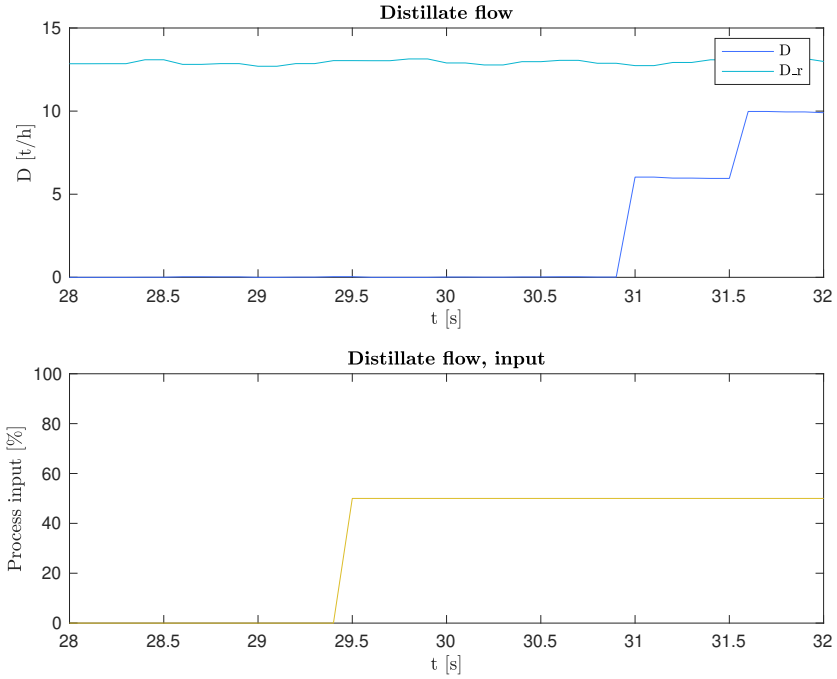

Fig. 27: Open-loop step response of D

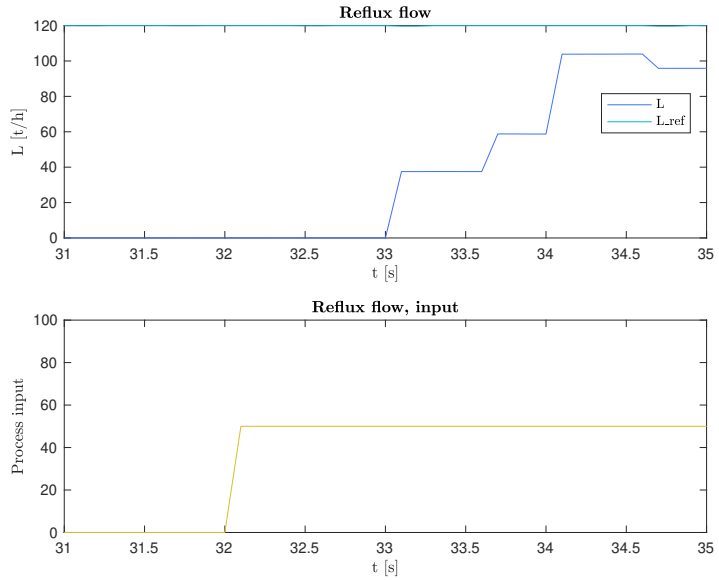

Fig. 28: Open-loop step response of L

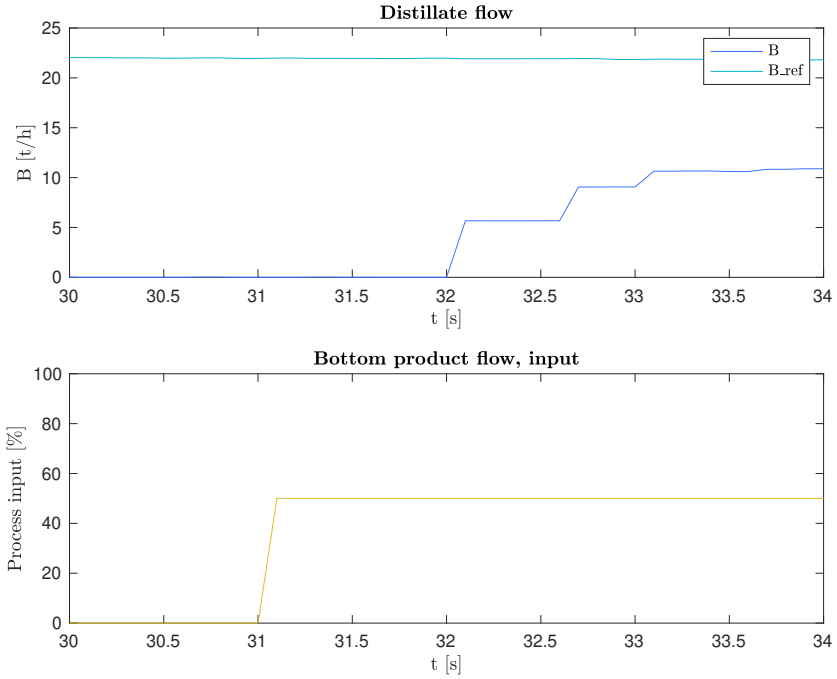

Fig. 29: Open-loop step response of B

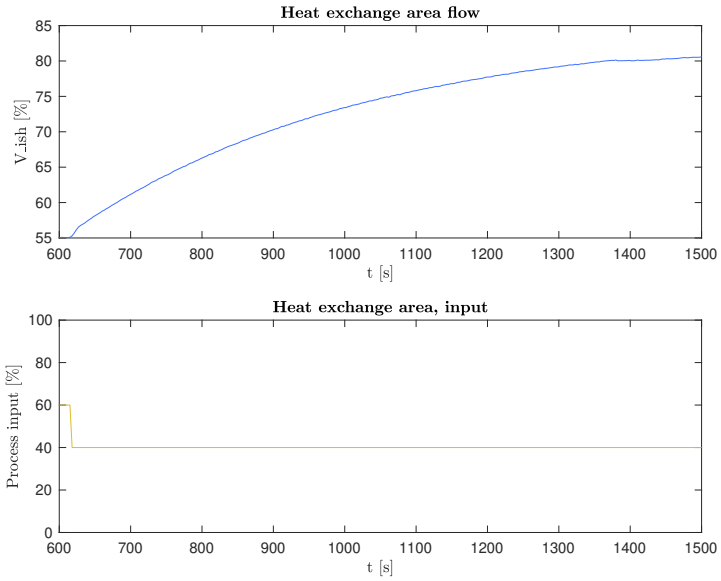

Fig. 30: Open-loop step response of heat exchanger area, related to V

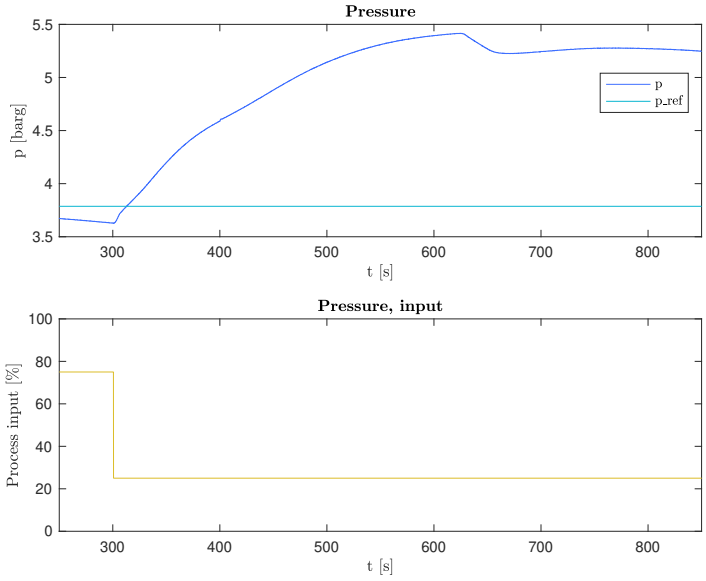

Fig. 31: Open-loop step response of p

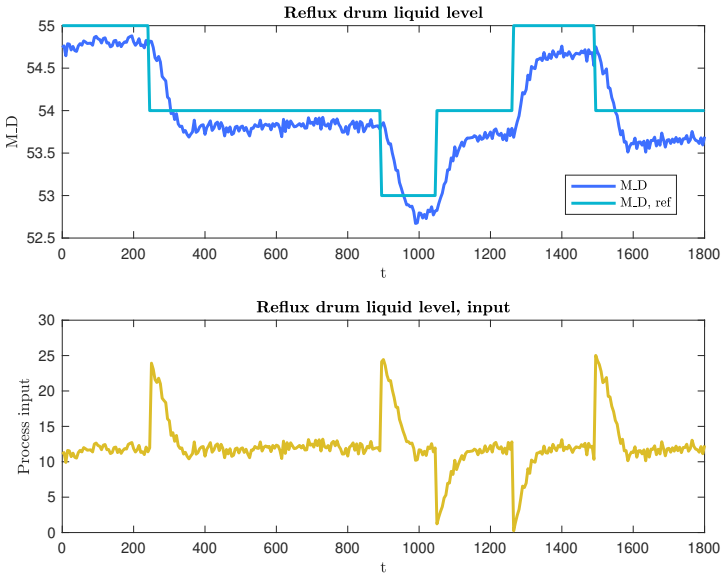

Fig. 32: System identification experiment for M_D controller

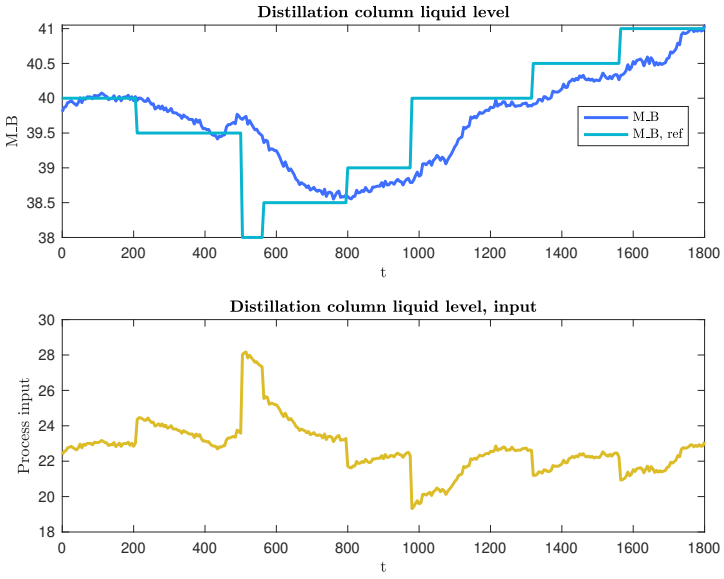

Fig. 33: System identification experiment for M_B controller

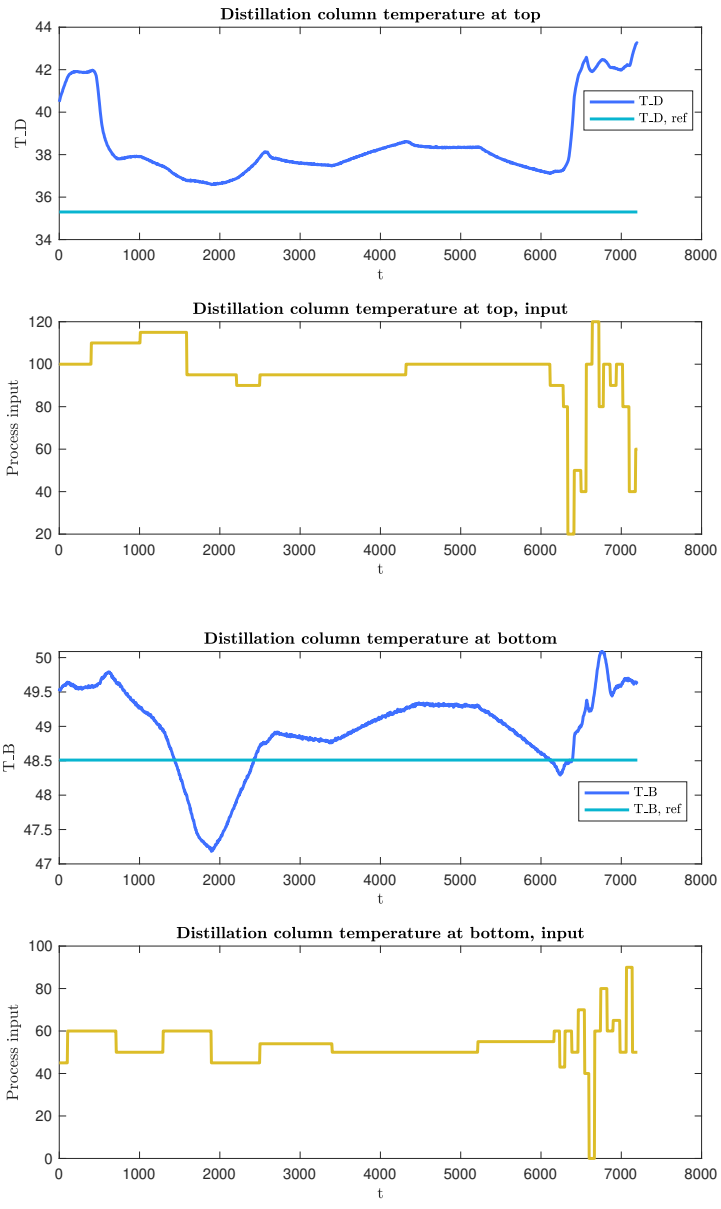

Fig. 34: Response of T_D and T_B to step changes in L and V